Hindawi Publishing Corporation
International Journal of Polymer Science
Volume 2016, Article ID 8690967, 12 pages
http://dx.doi.org/10.1155/2016/8690967

Research Article

Self-Shrinkage Behaviors of Waste Paper Fiber Reinforced Cement Paste considering Its Self-Curing Effect at Early-Ages

Zhengwu Jiang,[1] Xiuyan Guo,[1,2] Wenting Li,[1] and Qing Chen[1]

[1]*Key Laboratory of Advanced Civil Engineering Materials, Ministry of Education, Tongji University, Shanghai 200092, China*
[2]*School of Mechanical & Electrical Engineering, Jinggangshan University, Ji'an, Jiangxi 343009, China*

Correspondence should be addressed to Zhengwu Jiang; jzhw@tongji.edu.cn

Received 10 February 2016; Revised 8 April 2016; Accepted 27 April 2016

Academic Editor: Zhouyang Xiang

The aim of this paper was to study how the early-age self-shrinkage behavior of cement paste is affected by the addition of the waste paper fibers under sealed conditions. Although the primary focus was to determine whether the waste paper fibers are suitable to mitigate self-shrinkage as an internal curing agent under different adding ways, evaluating their strength, pore structure, and hydration properties provided further insight into the self-cured behavior of cement paste. Under the wet mixing condition, the waste paper fibers could mitigate the self-shrinkage of cement paste and, at additions of 0.2% by mass of cement, the waste paper fibers were found to show significant self-shrinkage cracking control while providing some internal curing. In addition, the self-curing efficiency results were analyzed based on the strength and the self-shrinkage behaviors of cement paste. Results indicated that, under a low water cement ratio, an optimal dosage and adding ways of the waste paper fibers could enhance the self-curing efficiency of cement paste.

1. Introduction

Because of the need of long spans, towering, and overloading and harsh conditions in modern engineering, the high-performance concrete (HPC) has been widely used in the infrastructure, such as bridges, high-rise buildings, port, and underground projects, due to the high strength and high performance [1, 2]. However, self-desiccation leading to self-shrinkage causes the early cracks of concrete, which have been recognized to be a major shortcoming of HPC [3–5].

Because of a low water-binder ratio of HPC, a large amount of unhydrated cement within concrete can attract water from the capillary and begin to hydrate. Yet external moisture is difficult to penetrate into the inside of the concrete due to the compacting concrete structure and the capillary dehydrates and forms a vacuum even, leading to the self-shrinkage of concrete. With the early hardening of concrete, the shrinkage deformation is greater than the ultimate stretching deformation, which always causes the cracking and then decreases the permeability and the carbonation resistance of concrete. Thus the self-desiccation shrinkage of concrete is closely related to the drop of its internal relative humidity; this is confirmed in the previous studies [6–8]. In order to effectively control and improve the self-shrinkage of concrete, an absorbent polymer as a self-curing agent is developed to improve the hydration degree of concrete and reduce the compressive stress and the sensitivity to cracking [9–11].

Cellulose fibers that owned the amorphous structure are evenly dispersed in concrete, which efficiently restrain crack formation and delay crack growth [12, 13]. In addition, cellulose fibers have a nature hydrophilic property [14], which plays a key role in the concrete. Internal curing is explored from water-saturated porous cellulose fibers to provide additional curing water in the early hydration process of concrete. This strategy is effective because the additional curing water can replenish the emptying pores more quickly than traditional external curing water [15]. This process accelerates hydration of cement and then enhances the interfacial cohesiveness between cellulose fibers and cementing material, which increases the compactness, improves the permeability resistance of concrete, and gives the concrete better durability and service life [16].

Waste paper fibers (WPFs) are affiliated with cellulose fibers and have their advantages, such as an amorphous

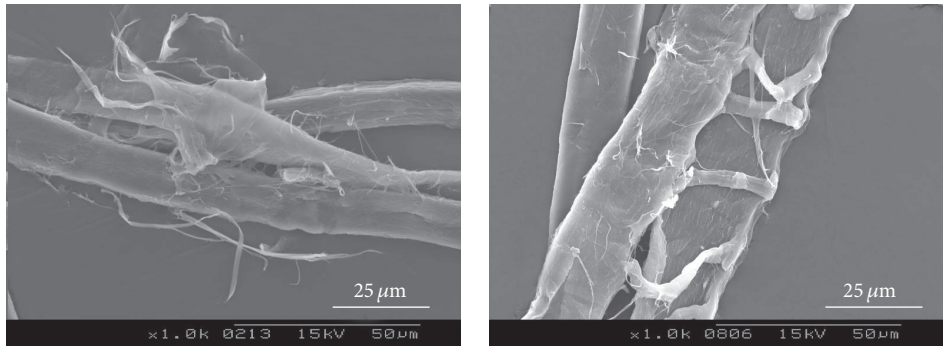

(a) (b)

Figure 1: SEM surface morphologies of WPFs.

Table 1: Chemical component of the waste paper fibers (wt%).

Component	Cellulose	Hemicellulose	Fillers
Content (%)	~93	~5	~2

structure and a nature hydrophilic property [17]. Theoretically speaking, the WPFs can be used as a substitute for the cellulose fibers and applied in concrete. Moreover, the WPFs used in concrete do not require the use of the deinking and bleaching processes, thereby greatly reducing the emissions of hazardous substances in the wastewater [18]. Previous studies had shown that cheap WPFs could enhance the concrete [19] and reduce the dosage of cement [20]; the mechanical property and the durability of the WPFs concrete were also researched [21]. However, the use of the WPFs to enhance the shrinkage resistance and self-curing effect of concrete has not been yet reported. This research aims to contribute to filling this lack of knowledge.

It is generally known that the shrinkage of concrete is influenced by many factors except low water ratios; in order to truly reflect the self-shrinkage and self-curing behaviors of the WPFs reinforced cement-based materials, the cement paste instead of concrete is selected as the matrix which does not consider other factors. The self-shrinkage and self-curing behaviors of cement paste with the WPFs are researched in this paper. In addition, the reasonable addition ways and dosage of WPFs in cement paste at a low water cement ratio are discussed, which can provide theoretical basis for actual production.

2. Experimental

2.1. Materials. Waste paper fibers (WPFs) from newsprint were pretreated and modified surfaces in our own lab [22]. They have an average length of 1.6 mm, an average diameter of 24 μm, and a specific surface area of 2.3 m^2/g. The chemical content of the WPFs was listed in Table 1. From the chart, the content of cellulose was about 93%, showing that the WPFs owned good alkali resistance. The SEM surface morphologies of WPFs were shown in Figure 1. The fiber bundle was layered along the long end; many microfibrils were produced and exist on the fiber surfaces (Figure 1(a)), and the WPF that owned porous hollow structure was shown quite clearly (Figure 1(b)), which allows it to absorb and retain water.

A Portland cement P.II 52.5 and tap water were used in all mixes, a polycarboxylic high-performance water-reducing agent (SD-600P-01) was used to adjust the workability of cement paste, and the fluidities of all the samples were controlled at 140 ± 10 mm. The chemical compositions of clinker were listed in Table 2.

2.2. Mix Design. All the mixtures were designed to have a fluidity indice of 140 ± 10 mm. Two main differences between the mixes were the dosage and the adding ways of the WPFs. The dosages of the WPFs were 0.1%, 0.2%, 0.3%, and 0.4% by mass of cement, respectively. Wet mixing and dry mixing were implemented at a water cement ratio of 0.3. Among them, wet mixing was that both the WPFs and the total quotas of water were weighed firstly, and then the fibers were soaked in the normed water at least 30 min until the WPFs were treated to be fully dispersible in water, at which point this mixture was mixed with cement. However, dry mixing was that the preweighed dry WPFs were mixed with cement firstly, and then suitable water was added to compound. The mix designs of cement pastes were shown in Table 3.

2.3. Testing Methods. To improve the testing accuracy, three same specimens of every curing age were prepared and tested for each sample, as described below.

2.3.1. Compressive Strength and Flexural Strength. According to the Chinese National Standard GB/T 17671-1999 [23], cement pastes were casted in 40 mm × 40 mm × 160 mm molds and vibrated at the time of casting to remove air bubbles. The molded pastes were kept at temperature 20 ± 2°C and relative humidity exceeding 95% for 24 h and then removed from the molds. The demoulded samples were sealed with high density polypropylene film and epoxy resin sealant and then cured in a room with temperature 20°C and relative humidity 60% for the set ages. The compressive and flexural strengths of all specimens were determined using a ACE-201 strength test machine. Three same specimens of every curing age were measured and the arithmetic average

Table 2: Chemical components of clinker (wt%).

Components	SiO_2	Al_2O_3	Fe_2O_3	CaO	MgO	SO_3	K_2O	Na_2O	Total
Content (%)	21.74	5.06	3.56	66.6	0.88	0.81	0.55	0.05	99.25

Table 3: Mix proportion of cement paste.

Code	W/C	Water/(kg/m^3)	Cement/(kg/m^3)	Superplasticizer (by mass of cement)/‰	WPFs dosage (by mass of cement)/%	WPFs adding way
A0	0.25	200	800	2.8	—	—
A1	0.25	200	800	3.5	0.1	Wet mixing
A2	0.25	200	800	4.2	0.2	Wet mixing
A3	0.25	200	800	5	0.3	Wet mixing
A4	0.25	200	800	5.8	0.4	Wet mixing
B0	0.3	240	800	1.8	—	—
B1	0.3	240	800	2.2	0.1	Wet mixing
B2	0.3	240	800	2.8	0.2	Wet mixing
B3	0.3	240	800	3.5	0.3	Wet mixing
B4	0.3	240	800	4.4	0.4	Wet mixing
B5	0.3	240	800	3	0.2	Dry mixing

was taken as the ultimate strength of cement paste. Based on these data, the compressive to flexural strength (σ_C/σ_F) was calculated. Finally, the central parts of specimens were dried and stored in alcoholic solution for micro measurements.

2.3.2. Self-Shrinkage Characteristics. According to the Chinese National Standard JGJ/T 70-2009 [24], all specimens were casted in the 40 mm × 40 mm × 160 mm shrinkage molds and shocked slightly at the time of casting to remove air bubbles. The molded specimens were kept at 20 ± 2°C and relative humidity exceeding 95% for 24 h and then removed from the molds and measured length (L_0). All specimens were sealed and cured under the same conditions as those mentioned above. The length of specimen cured for each age (L_t) was measured. The linear shrinkage strain of cement paste was determined according to

$$\varepsilon_{at} = \frac{L_0 - L_t}{L - L_d}, \tag{1}$$

where ε_{at} is the linear shrinkage ratio of specimen cured for t days ($t = 1, 3, 7, 28, 56, 90$); L_0 is the initial length of specimen with feeder head; L_t is the actual length of specimen cured for t days ($t = 1, 3, 7, 28, 56, 90$); L is the length of specimen (160 mm); and L_d is the sum length of two feeder heads buried in the specimen.

2.3.3. Hydration Characteristics

(1) TG-DSC. The contents of calcium hydroxide in the hardened cement paste were assessed by a thermogravimetry-differential scanning calorimetry (TG-DSC). To do so, the specimens were dried at 40°C for approximately 24 h; these dried specimens were crushed, pestled, and sieved, and small particles ranging from 200 μm to 500 μm were collected as samples. In a thermal analysis, about 30 mg of a sample was put in an alumina top-opened crucible and heated from room temperature to 850°C at a rate of 10°C/min. The weight loss data and energy compensation data were determined and recorded for further analysis. Nitrogen gas was chosen as the dynamic atmosphere and corundum as the reference material.

The hydration degree of cement paste was quantitatively calculated by the thermal analysis. The following was the calculating method [25]:

$$G_t\,(\mathrm{CH}) = \frac{\Delta m}{m_0} \times \frac{M_{\mathrm{CH}}}{nM_{\mathrm{loss}}} \times 100\% \tag{2}$$

$$\mathrm{Ca(OH)_2} \longrightarrow \mathrm{CaO} + \mathrm{H_2O} \tag{3}$$

where Δm is the loss of quality in the calculating temperature range; m_0 is the original quality; M_{loss} and M_{CH} are the molecular weights of the loss of gas (H_2O) and predicted component ($Ca(OH)_2$), respectively; and n is the mole number of lost gas in one mole sample ($n = 1$).

(2) XRD. Mineral phases of cement pastes were identified by a D/max 2550VB3/PC* X-ray powder diffractometer (XRD). All samples were prepared as described above. The patterns produced using Cu-K-α radiation ($\lambda = 0.15418$ nm) at 40 kV and 100 mA were recorded in the range of 2θ at 5°~70°, in 0.02° steps, counting by 4 s per step.

2.3.4. Pore Structure. The pore structure of cement paste was determined by a mercury intrusion porosimeter (Poremaster GT-60). Pore size is related to the pressure by Washburn's equation, which assumes that the pores have circular cross sections:

$$P = \frac{-2\sigma' \cos\theta}{r}, \tag{4}$$

Table 4: The strengths of cement pastes at a different water cement ratio for sealed curing.

Code	W/C	WPF (%)	Flexural strength (MPa)					Compressive strength (MPa)					σ_C/σ_F				
			1 d	3 d	7 d	28 d	90 d	1 d	3 d	7 d	28 d	90 d	1 d	3 d	7 d	28 d	90 d
A0	0.25	—	10.9	11.6	10.8	8.1	17.5	72.6	88.2	90.3	104.4	113.8	6.64	7.59	8.3	12.8	6.5
A1	0.25	0.1	11.4	12.5	11.3	10.1	16.8	74.6	89.0	91.4	107.3	115.9	6.55	7.13	8.1	10.6	6.9
A2	0.25	0.2	11.8	13.2	12.9	12.6	16.5	76.9	89.4	95.0	108.0	120.5	6.5	6.8	7.3	8.6	7.3
A3	0.25	0.3	10.2	12.5	12.0	10.6	15.1	73.8	85.9	94.0	100.9	110.4	7.27	6.9	7.8	9.5	7.3
A4	0.25	0.4	8.7	9.8	9.7	9.1	14.8	71.1	82.2	86.9	94.2	103.6	7.7	8.4	8.9	10.3	7
B0	0.3	—	6.6	7.5	9.0	10.2	11.4	49.4	73.5	82.0	89.4	93.5	7.5	9.8	9.1	8.8	8.2
B1	0.3	0.1	6.0	7.7	9.5	10.4	9.9	42.0	69.4	77.8	87.1	91.5	7	9.1	8.2	8.4	9.2
B2	0.3	0.2	5.9	9.1	9.3	9.8	9.2	33.1	67.9	72.2	81.0	86.4	5.6	7.5	7.8	8.3	9.4
B3	0.3	0.3	5.6	8.6	8.9	9.2	8.5	31.2	67.6	71.8	80.0	82.1	5.6	7.9	8.1	8.7	9.7
B4	0.3	0.4	5.5	6.6	7.1	8.9	6.5	29.3	65.4	69.7	79.6	74.8	5.3	9.8	9.8	11.1	11.6

where P is the pressure exerted (N/m^2); r is the pore radius (μm); σ is the surface tension of mercury (N/m^2); and θ is the contact angle (°).

In this study, a maximum pressure of 14×10^8 N/m^2 was applied. The surface tension σ of 0.480 N/m and the contact angle (θ) of 140° were used for the calculation of pore size.

Small pieces of cement paste weighing 1.2 g obtained from the middle part of 60 mm cement paste specimens were used for Mercury Intrusion Porosimetry (MIP) testing. In order to stop the hydration, the specimens were dried at 105°C for approximately 24 h until a constant weight was achieved, and then they were kept in sealed containers until the day of the test. Two MIP tests were conducted for each sample, and the average values of the MIP results were used for data comparison.

3. Results and Discussion

3.1. Strength. Cement-based material is typical heterogeneous brittle materials; shrinkage cracking is one of the significant factors of its failures. To improve its brittleness, toughness is especially important. The σ_C/σ_F is one of the toughness indices of materials; the lower the σ_C/σ_F, the better the toughness and the stronger the shrinkage resistance of materials.

3.1.1. The Effect of the WPFs Dosage on Strength. WPFs were mixed with cement using wet mixing, dealing with strength, and compressive to flexural strength ratio σ_C/σ_F of samples is as shown in Table 4.

At water cement ratio of 0.25, the flexural strengths of all samples increased in the first three days and then decreased gradually with curing age, and the decline degrees of flexural strengths were different. After curing for 28 d, the flexural strengths of all samples were greatly raised. The flexural strength of cement paste is influenced by hydration and water cement ratio. In principle, the lower the water cement ratio and the quicker the hydration process, the higher the flexural strength. The WPF has mainly an impact on the flexural strength of cement paste because of its absorbing and releasing moisture. Before sealed curing for 3 d, the humidity dropped down and more gels were formed with hydration, which made the flexural strength of specimen increase. However, after curing for 3 d, once the negative pressure water supply occurred, the WPF would release water to compensate it. The actual water cement ratio increase caused by release moisture was likely to play a leading role. On the one hand, moisture from WPFs promoted the hydration process and improved the flexural strength further; on the other hand, it is just because released moisture increased the actual water cement ratio, causing the reduction of the flexural strength; these two contradictory factors caused the decrease of the flexural strength of specimen cured for 3–28 d. After curing for 28 d, the hydration forced the rapid water loss of WPFs and formed more hydration products, which caused the rapid growth of the flexural strength. When the dosages of the WPFs were 0.1%~0.3% by mass of cement, the flexural strengths of cement pastes cured for 3 d~28 d were higher than those of control samples. Among them, the dosage of the WPFs was 0.2% by mass of cement and the flexural strength of cement paste cured for 28 d was significantly the highest and increased by 55.6%. However, when the dosage of the WPFs was 0.4%, the flexural strengths of cement pastes were obviously lower than those of control samples except 28 d, and thus, under the quantity, the WPFs had a negative effect on the flexural strength. At the same water cement ratio, the compressive strengths of cement pastes increased with the dosage of the WPFs and reached highest at the dosage of 0.2%. However, the flexural strengths of cement pastes were slightly larger than those of control samples when water cement ratio was 0.3 and the dosage of the WPFs was less than 0.2%. Besides, the flexural strength and the compressive strength of cement paste decreased with the dosage of the WPFs.

Whatever water cement ratios, when the dosage of the WPFs was 0.1%~0.3% by mass of cement, the σ_C/σ_F of cement paste cured for 3 d~28 d was lower than that of standard sample. When a water cement ratio was 0.25, the σ_C/σ_F of cement paste containing 0.2% WPFs was lowest and dropped by more than 30 percent when cement paste was cured for 28 d; as for the WPFs dosage of 0.3%, the σ_C/σ_F of cement paste cured for 1 d was higher than that of standard sample, which could be because of experimental mistakes. However, when cement paste was cured for 90 d, the σ_C/σ_F of cement

Table 5: The strengths of cement pastes at a water cement ratio of 0.3 for sealed curing.

Code	WPFs (%)	Adding ways	Flexural strength (MPa)					Compressive strength (MPa)					σ_C/σ_F				
			1 d	3 d	7 d	28 d	90 d	1 d	3 d	7 d	28 d	90 d	1 d	3 d	7 d	28 d	90 d
B0	—	—	6.6	7.5	9.0	10.2	11.4	49.4	73.5	82.0	89.4	93.5	7.5	9.8	9.1	8.8	8.2
B2	0.2	Wet mixing	5.9	9.1	9.3	9.8	9.2	33.1	67.9	72.2	81.0	86.4	5.6	7.5	7.8	8.3	9.4
B5	0.2	Dry mixing	5.3	7.7	8.7	9.0	8.4	47.5	64.3	86.0	87.3	82.5	8.9	8.3	9.9	9.7	9.9

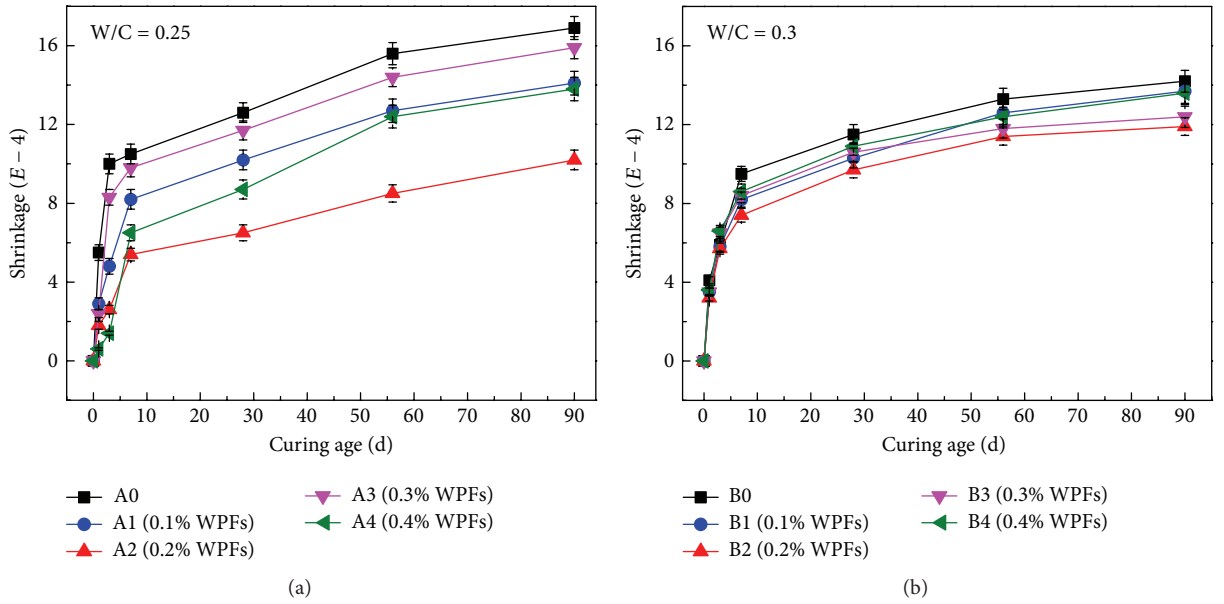

Figure 2: The shrinkages of cement pastes at a water cement ratio of 0.25 (a) and 0.3 (b).

paste containing WPFs was higher than that of standard sample, which means that, with the dosage of 0.1%~0.3% by mass of cement, the WPFs were able to improve the toughness of cement paste cured for early-age. The lower the water cement ratio, the better the WPFs improving the toughness of cement paste. In addition, when the dosage of the WPFs was 0.2% by mass of cement, the toughness of cement pastes cured for early-age was optimal.

3.1.2. The Effects of the WPFs Adding Ways on Strength. At water cement ratio of 0.3, the WPFs of 0.2% by mass of cement were mixed with cement using wet mixing and dry mixing, respectively. The strength and the σ_C/σ_F of cement pastes are as shown in Table 5.

Throughout these data in Table 5, the values of compressive strength had no obvious variety regulation, but when the WPFs were added with wet mixing, the flexural strengths of cement pastes (B2) were higher than those of dry mixing (B5). From σ_C/σ_F, we found that σ_C/σ_F of sample B2 cured within 28 days was lower than those of B0 and B5, which showed that the WPFs could improve the toughness of cement paste, but the degree of improvement was about the adding ways of WPFs. The adding ways of the WPFs directly affected the dispersion degree of fibers and then affected the performance of cement paste. It was difficult to disperse WPFs in the condition of dry mixing, causing WPFs to agglomerate in matrix, which was unfavorable to improve the toughness of cement paste. Thus, compared with dry mixing, the adding way of WPFs with wet mixing was suitable.

3.2. Shrinkage Characteristics

3.2.1. The Effect of Fiber Dosage on the Self-Shrinkage. It is widely understood that adding cellulose fiber to cement-based materials can control the drying shrinkage cracking and the plastic shrinkage [26–28]. In addition, cellulose fibers can be dispersed in hydrating cement paste and have the capacity to absorb and release water to enhance the internal curing and inhibit the self-shrinkage of cement paste [15]. Figure 2 gives an overview on how the WPFs dosages affect the shrinkage of cement paste at different water cement ratios.

Figure 2(a) shows that the WPFs effectively decreased the shrinkage of cement paste at a water cement ratio of 0.25. As mentioned previously, the WPFs belong to the cellulose fibers, which could absorb some water and maintain saturated state before being mixed with cement. The humidity of matrix gradually dropped with the hydration of cement; at this point, the WPFs would release moisture to compensate it and promote the hydration further. More hydration gels were generated and growing along the surface of the WPFs-like bridge, which enhanced the strength and the shrinkage resistance. However, the reinforcing effects related to the

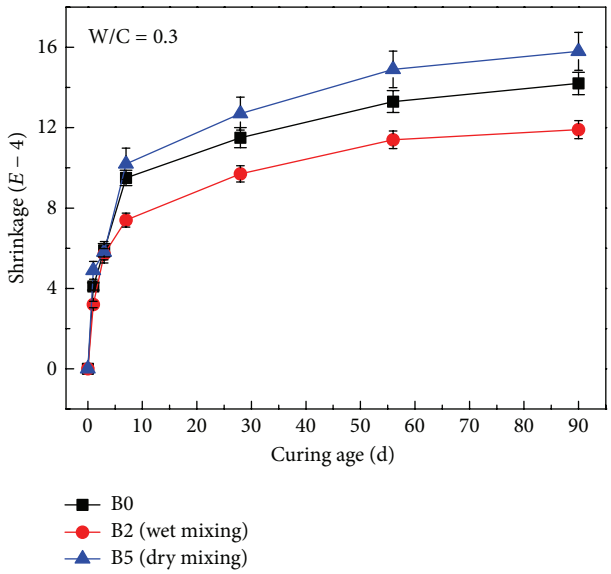

Figure 3: The shrinkage of cement paste containing WPFs using different adding ways.

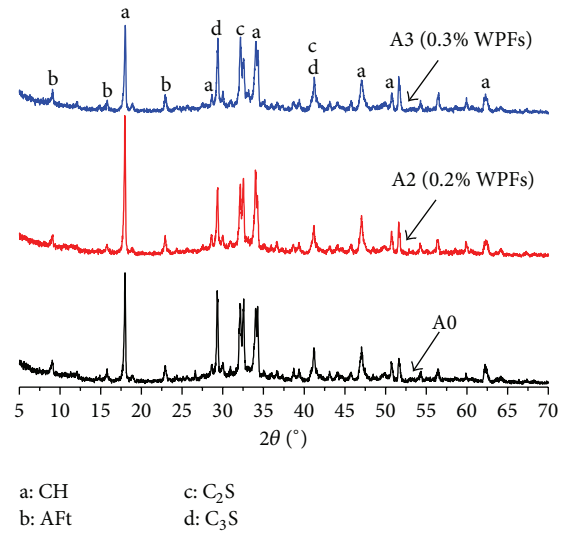

Figure 4: XRD patterns of cement pastes at a water cement ratio of 0.25.

dispersion of the WPFs. Smaller amounts of the WPFs have no effect on antishrinkage, while bigger amounts of the WPFs were not distributed in cement paste well, causing the weaker antishrinkage. When the dosage of the WPFs was 0.2% by mass of cement, the shrinkage of cement paste was lowest. The shrinkage of cement paste cured for 1 d decreased by 67% based on control sample, and when cement paste was cured for 3 d and 7 d, the shrinkages of cement paste were decreased by 74% and 50%, respectively. Although the shrinkage of cement paste containing 0.4% WPFs was also lower, the flexural strength of this sample decreased by about 30% when it was cured for 3 days (Table 3), causing the negative impact on paste, so excessive amounts of WPFs were improper.

Compared with Figure 2(a), although adding the WPFs to cement paste reduced the shrinkage of paste, the effect was obviously smaller at a water cement ratio of 0.3 (Figure 2(b)). When the WPFs dosage was 0.2% by mass of cement, similarly, the cement paste had a minimum linear shrinkage strain. When cement paste was cured for 1 d and 3 d, its shrinkage was decreased by 22.0% and 22.1% based on control sample, respectively.

Taken together with the σ_C/σ_F and the shrinkage of cement paste, the WPFs dosage of 0.2% by mass of cement is optimal in either water cement ratio, which improved the toughness and antishrinkage of cement paste. However, it is easy to see that the lower the water cement ratio, the better the antishrinkage capability of the WPFs in cement paste.

3.2.2. The Effects of Fiber Adding Ways on the Self-Shrinkage. The WPFs dosage of 0.2% by mass of cement was mixed with cements using wet mixing and dry mixing, respectively. The linear shrinkage strain is shown in Figure 3. The WPFs were mixed with cement using dry mixing way, which increased the shrinkage of cement paste. However, using wet mixing, the WPFs decreased the shrinkage of cement paste. This illustrates that the WPFs adding way of wet mixing was better than that of dry mixing even with the same content of WPFs.

3.3. Hydration Characteristic. $Ca(OH)_2$ is an important hydration product of cement-based materials. Some properties of cement-based materials, such as carbonation resistance and alkalinity, are about the content of $Ca(OH)_2$. A fast rate for carbonation caused by low levels of $Ca(OH)_2$ leads to the decrease of pH, inducing the corrosion of rebar in cement-based materials [29, 30]. So some levels of $Ca(OH)_2$ in cement-based materials are necessary but not sufficient condition for durability.

The crystalline phase compositions of cement pastes cured for 7 d were identified by XRD, and their XRD patterns are given in Figure 4. In addition to the typical characteristic peaks of C_2S and C_3S, the cement hydration product $Ca(OH)_2$ was found in all specimens. Although the diffraction peak intensity was not directly proportional to the content of crystalline phase, some important information can be obtained from comparisons of the relative intensity of $Ca(OH)_2$. When cement paste was cured for 7 days, it was found that the diffraction intensity which was in $Ca(OH)_2$ peak at about 18° of cement paste containing 0.2% WPFs was significantly higher than control sample and cement paste containing 0.3% WPFs; it showed that more hydration products were formed in cement paste containing 0.2% WPFs.

To further confirm the content of $Ca(OH)_2$ in the hydration products, the losses of quality of cement pastes cured for 7 d are analyzed. TG-DSC patterns of the standard sample and the cement paste containing 0.2% WPFs cured for 7 d are shown in Figure 5.

From Figure 5, there was an endothermic peak near 440°C in the DSC curve of cement paste, which resulted from the dehydration of structural water from $Ca(OH)_2$ [31]. According to the loss of quality in the TG curve of paste, the content of $Ca(OH)_2$ in hydration products was calculated

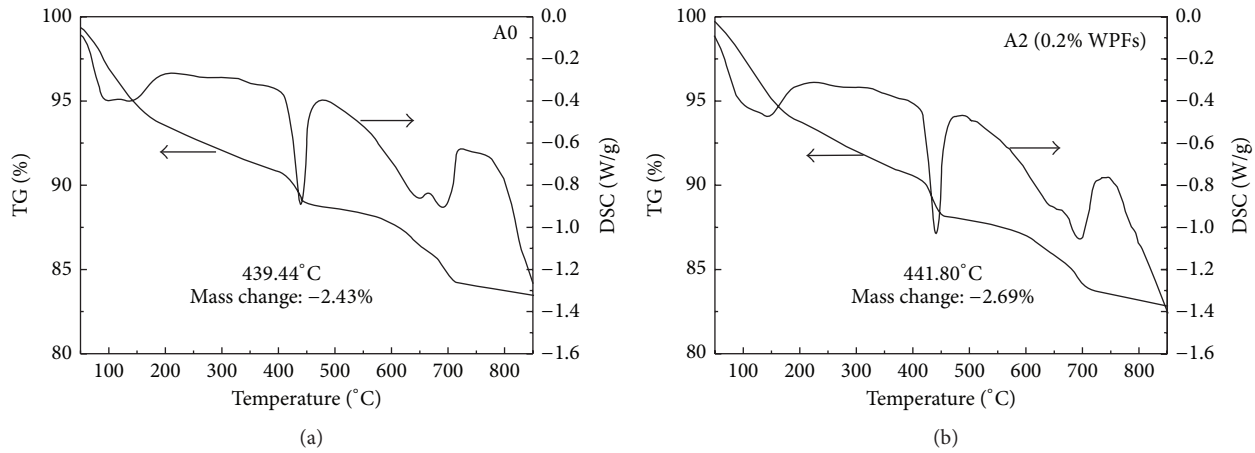

Figure 5: TG-DSC patterns of cement pastes cured for 7 d at a water cement ratio of 0.25.

Table 6: The content of $Ca(OH)_2$ of cement pastes under different conditions.

Project	W/C	Adding dosage (%)	Curing age (d)	Mass change (%)	$Ca(OH)_2$ (%)
A0	0.25	—	7	−2.43	9.99
A1	0.25	0.1	7	−2.48	10.20
A2	0.25	0.2	7	−2.69	11.06
A3	0.25	0.3	1	−2.24	9.21
A3	0.25	0.3	7	−2.51	10.32
A3	0.25	0.3	28	−2.67	10.98
A4	0.25	0.4	7	−2.50	10.28
B0	0.3	—	7	−2.83	11.63
B2	0.3	0.2	7	−2.87	11.80
B5	0.3	0.2	7	−2.85	11.72

B5: dry mixing; other samples: wet mixing.

and listed in Table 6. The content of $Ca(OH)_2$ in hydration products continuously increased with the dosage of WPFs. When the WPFs dosage was 0.2% by mass of cement, the content of $Ca(OH)_2$ of cement paste cured for 7 d increased to 11.06% from 9.99%. However, if the WPFs dosage continued to increase, the content of $Ca(OH)_2$ in hydration products decreased instead. In addition, when a water cement ratio was 0.3, the content of $Ca(OH)_2$ in hydration products increased with the curing age. When the cement pastes were identical in the water cement ratio, the WPFs dosage, and curing age, the content of $Ca(OH)_2$ in hydration products was different because of the WPFs adding ways. The content of $Ca(OH)_2$ was higher in cement paste which mixed with WPFs using wet mixing than that of using dry mixing.

3.4. Pore Structure. The compactness of cement-based materials is closely related to mechanical property and antishrinkage. The pore size distribution and pore volume are inevitable to change with the hydration process of cement paste. The WPFs have different effect on pore structure of cement-based materials. The mercury cumulative intrusion curves and their derivatives are shown in Figure 6.

From Figure 6(a), when cured for 7 d, the cumulative intrusion of paste containing WPFs was lower than that of paste without fibers, among them, when adding 0.2% WPFs, the cumulative pore volume of cement paste was lowest. Adding the same dosage of the WPFs, the cumulative intrusion of cement paste decreased with the curing age (Figure 6(b)). The cumulative porosity of cement paste cured for different ages is shown in Table 7. With a water cement ratio of 0.25 and curing for 7 d, whatever WPFs dosage, the total porosity of sample decreased. In addition, the percentages of the pore which was smaller than 50 nm and the pore which was greater than 100 nm in the total porosity increased and decreased, respectively. Among them, the total porosity of the sample containing 0.2% WPFs decreased by 2.59% over the control sample. When the W/C and the WPFs dosage were same, the total porosity of sample decreased with the curing age; the total porosities of cement pastes cured for 7 d and 28 d decreased by 4.42% and 7.72% over cured for 1 d, respectively. With a water cement ratio of 0.3, the total porosity of paste which mixed with the WPFs using wet mixing decreased obviously in comparison with two other samples.

3.5. Self-Curing Efficiency

3.5.1. The Proposing of Self-Curing Efficiency. Through the above analysis, the WPFs could enhance toughness and self-shrinkage of cement paste. Supporting the cement paste without the WPFs as control sample, the flexural strength, compressive strength, and linear shrinkage strain were σ_{F0}, σ_{C0}, and ε_0, respectively. Those of the cement paste with WPFs were σ_{Ff}, σ_{Cf}, and ε_f, respectively. Now drawn up η (%) as the self-curing efficiency of WPFs enhanced cement paste, in which η_1 was strength efficiency, including flexural strength efficiency η_{F1} and compressive strength efficiency η_{C1} and η_2 was shrinkage efficiency. η_1 was the ratio of the reduction of

Table 7: Cumulative porosity of cement paste under different conditions.

Code	W/C	Adding dosage (%)	Curing age (days)	Cumulative porosity (%)			
				<50 nm	50 nm~100 nm	>100 nm	Total porosity
A0	0.25	—	7	4.45	8.66	3.02	16.13
A1	0.25	0.1	7	4.34	8.36	2.25	14.95
A2	0.25	0.2	7	4.42	8.24	0.88	13.54
A3	0.25	0.3	1	6.10	8.99	3.85	18.94
A3	0.25	0.3	7	3.70	8.76	2.06	14.52
A3	0.25	0.3	28	2.23	7.56	1.43	11.22
A4	0.25	0.4	7	3.36	9.29	2.71	15.36
B0	0.3	—	7	6.15	7.84	5.22	19.21
B2	0.3	0.2	7	6.03	6.22	3.95	16.13
B5	0.3	0.2	7	6.34	7.43	4.89	18.66

B5: dry mixing; other samples: wet mixing.

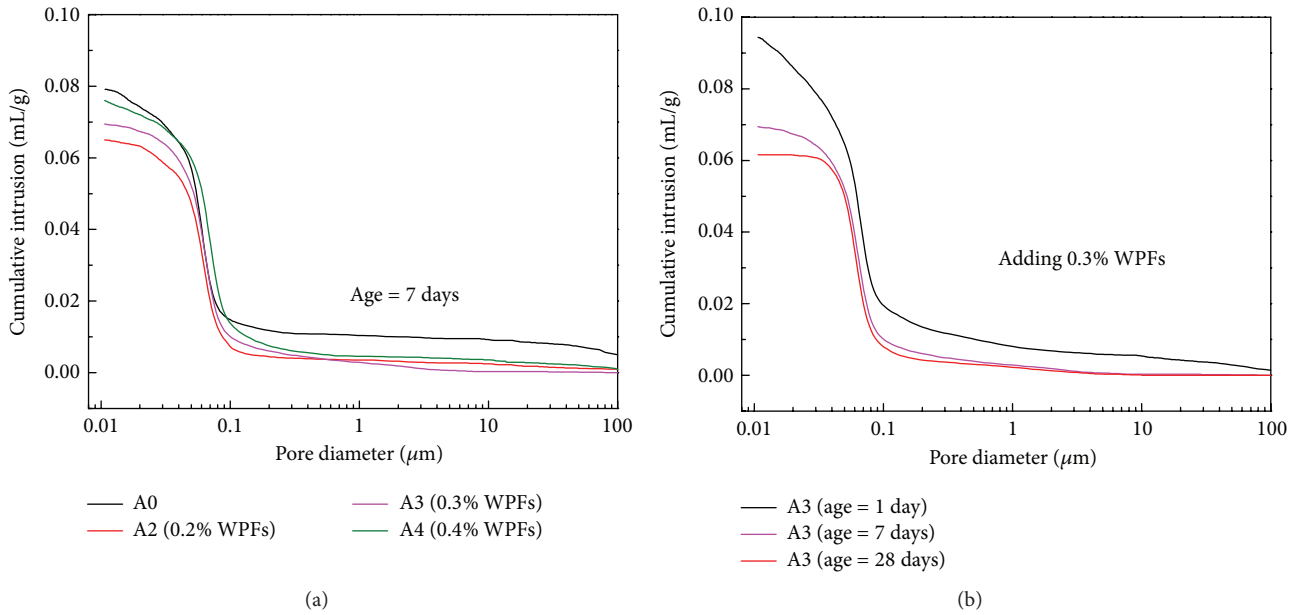

Figure 6: Cumulative intrusion of cement paste at a water cement ratio of 0.25.

relative strength to reference strength and η_2 was the ratio of the reduction of linear shrinkage strain to reference shrinkage strain, as shown in the following formula:

$$\eta_{F1} = \frac{\sigma_{Ff} - \sigma_{F0}}{\sigma_{F0}} \times 100\%,$$
$$\eta_{C1} = \frac{\sigma_{Cf} - \sigma_{C0}}{\sigma_{C0}} \times 100\%, \quad (5)$$
$$\eta_2 = -\frac{\varepsilon_f - \varepsilon_0}{\varepsilon_0} \times 100\%.$$

Suppose the WPFs are distributed evenly in the cement paste; pore systems of the prewetting WPFs and cement paste should be considered as a whole. Moisture also transfers from the large pores to tiny pores, the pore size of the WPFs is far greater than the porous size of cement paste, so the moisture from the WPFs migrates progressively to the cement paste. The more the moisture the WPFs contain, the more the moisture transfer and the slower the relative humidity decreases, so the capillary stress and shrinkage of cement paste are smaller and the self-curing efficiency of cement paste is higher.

3.5.2. The Model of Self-Curing Efficiency. According to the formulas (5), the self-curing efficiencies of cement paste were obtained, as shown in Figure 7. Only $\eta > 0$; the WPFs were effective for the improvement of cement paste.

When water cement ratio was 0.25, WPFs could be able to enhance the self-curing efficiency of cement paste. From Figure 7(a), the flexural strength efficiency of the WPFs enhanced cement paste was best when the dosage of the WPFs was 0.2% by mass of cement. When cured for 7 d and 28 d, the flexural strength efficiencies of cement paste were increased by 19% and 56%, respectively. This means that the WPF gradually released moisture from itself and promoted

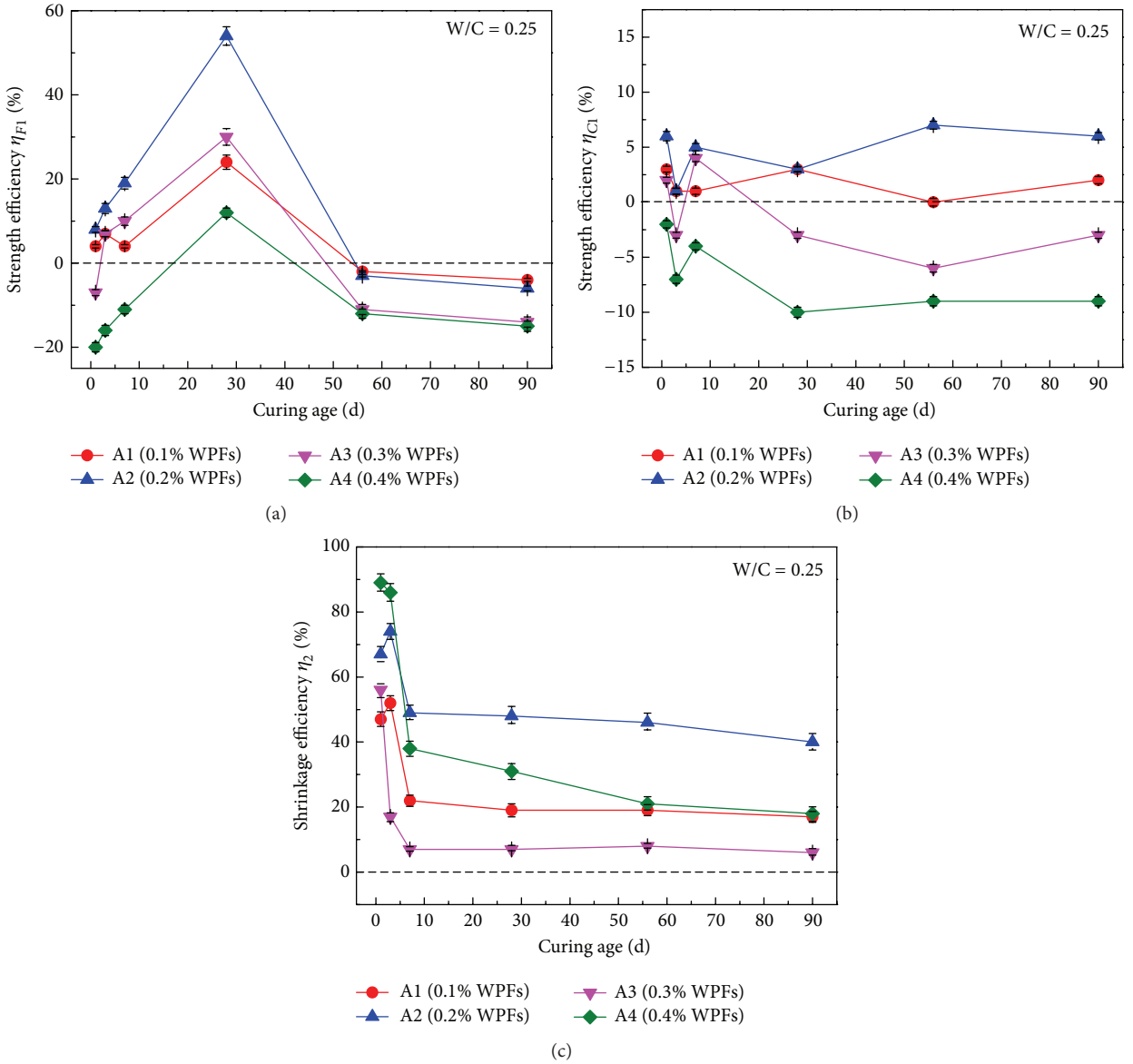

FIGURE 7: Self-curing efficiency of cement paste with WPFs at a water cement ratio of 0.25. (a) Flexural strength efficiency η_{F1}, (b) compressive strength efficiency η_{C1}, and (c) shrinkage efficiency η_2.

the hydration of the cement paste. However, the compressive strength efficiency η_{C1} of WPFs enhanced cement paste was not obvious (Figure 7(b)). The shrinkage efficiencies of the cement paste with 0.2% WPFs cured for 1 d and 3 d were improved 67% and 74%, respectively. When cement was cured for 7 d, the shrinkage efficiency was improved 50% or so (Figure 7(c)).

Taking part of samples, nonlinear fitting η_{F1}, η_{C1}, and η_2 using least square method, the multiple regression equation about η and the dosage of WPFs x was obtained, as shown in Table 8.

According to the fiber spacing theory [32], the fiber is equal to the secondary reinforcement and can be evenly dispersed in concrete, which hinders the development of microcrack; thus the concrete structure is more compact. In addition, it is generally known that some moisture will be consumed during the hydration process of cement. Without external water in a sealed environment, the water that the hydration reaction needs comes mainly from internal water of paste, so a water cement ratio is one of the most important factors in the hydration reaction and the shrinkage of cement paste [33, 34]. The WPF is a type of cellulose fiber, which plays a fiber bridge role in cement paste and improves the interface bonding state. Besides, the WPFs that owned porous structures (Figure 1) act as a storage reservoir, which can absorb and store moisture during mixing with cement, leading to the decrease of the effective water cement ratio. With the hydration reaction, water consumption causes self-desiccation of capillary in concrete [35]; just then the WPF releases moisture from itself to compensate the capillary and

Table 8: The regression equation of the self-curing efficiency of cement paste.

W/C	Age (d)	Self-curing efficiency η	Dosage of WPFs	R^2
0.25	1	$\eta_{F1} = -378.57x^2 + 100.43x - 0.3714$	$0 \le x \le 0.4$	0.9519
		$\eta_{C1} = -150x^2 + 55x - 0.2$	$0 \le x \le 0.4$	0.9239
		$\eta_2 = 5916.7x^3 - 3971.4x^2 + 864.4x - 1.1286$	$0 \le x \le 0.4$	0.9795
0.25	7	$\eta_{F1} = 1916.7x^3 + 621.43x^2 + 30.595x - 0.6714$	$0 \le x \le 0.4$	0.937
		$\eta_{C1} = -833.33x^3 + 335.71x^2 - 10.952x - 0.0857$	$0 \le x \le 0.4$	0.9899
		$\eta_2 = 245x - 0.8333$	$x < 0.2$	0.9965
		$\eta_2 = 3650x^2 - 2245x + 352$	$0.2 \le x \le 0.4$	1
0.25	28	$\eta_{F1} = -985.71x^2 + 424.29x - 1.7143$	$0.2 \le x \le 0.4$	0.8758
		$\eta_{C1} = -185.71x^2 + 42.286x + 0.0857$	$0.2 \le x \le 0.4$	0.9888
		$\eta_2 = 240x - 1.6667$	$x < 0.2$	0.9857
		$\eta_2 = 3250x^2 - 2035x + 325$	$0.2 \le x \le 0.4$	1

maintain the pressure in capillary pore at higher levels during the early-age curing period of cement-based materials, accelerating the hydration reaction of cement. The self-curing efficiency of WPFs in cement paste is realized based on the above process. The lower the water cement ratio, the better the self-curing efficiency of cement pastes; this is in line with existing research results [36–38].

The dosage and adding ways of the WPFs directly affect the effective water cement ratio. Proper WPFs will release more moisture to promote the hydration and more C-S-H gels grow along the WPFs to fill the space caused by the WPFs dehydration. More capillary pores are replaced by gel pores, which decrease the total porosity of cement paste. However, with adding too little WPFs, the absorbable and releasable moisture of WPFs are limited, causing the self-curing effect to be ineffective. If there are too many WPFs or uneven dispersion by dry mixing, which absorb substantial quantities of water and reduce the water cement ratio in an indirect way, WPFs could not unevenly distribute in cement paste; the moisture from the WPFs is fail to long-distance transport in time, leading to a weakened self-curing efficiency of cement paste and a relatively low $Ca(OH)_2$ production. In addition, the WPFs volume contraction after releasing water causes a plenty of spaces between the WPFs and the cementing material. These spaces form some weak spots in stress state of cement paste, which have negative impact on strength and antishrinkage of cement paste.

Based on the analysis above, under a low water cement ratio, an optimal dosage and adding ways of the WPFs could enhance the self-curing efficiency of cement paste. In this text, adding 0.2% WPFs to cement paste and wet mixing ways are optimal.

4. Conclusions

This study discussed the fact that WPFs reinforced the self-curing behavior of cement paste. The important conclusions are summarized below.

Under a low water cement ratio and wet mixing ways, the WPFs can decrease σ_C/σ_F and improve the toughness of cement paste. The lower the water cement ratio, the better the toughness of cement paste. When a water cement ratio is 0.25 and the dosage of the WPFs is 0.2% by mass of cement, the flexural strengths and the σ_C/σ_F of cement pastes cured for 28 d increase by 55.6% and decrease by 30%, respectively.

The WPFs in cement paste could promote the hydration process, decrease the cumulative pore volume, and increase the self-curing efficiency of cement paste. When water cement ratio is low and the WPFs dosage is 0.2% by mass of cement, the $Ca(OH)_2$ diffraction intensity of cement paste cured for 7 d is significantly higher than other samples and increases to 11.06%.

The WPFs could enhance the self-curing efficiency of cement paste. When a water cement ratio was 0.25 and the dosage of the WPFs was 0.2% by mass of cement, the flexural strength efficiencies of cement paste cured for 7 d and 28 d were increased by 19% and 56%, respectively. The shrinkage efficiencies of the cement paste cured for 1 d and 3 d were improved 67% and 74%, respectively.

Competing Interests

The authors declare that they have no competing interests.

Acknowledgments

The authors gratefully acknowledge the financial supports provided by National Basic Research Program of China (973 Program: 2011CB013805), National Natural Science Foundation of China (51278360, 51078269), National Key Project of Scientific and Technical Supporting Programs of China (no. 2014BAL03B02, no. 2012BAJ20B02), the Specialized Research Fund for the Doctoral Program of Higher Education of China (no. 20130072110047), the science and technology program of Jiangxi province (GJJ150775), and the Fundamental Research Funds for the Central Universities.

References

[1] T. A. Hammer, "Mix design of high strength concrete, economic design and construction with high strength concrete," Brite EuRum Projet 5480, SINTEF Structures and Concrete, 1994.

[2] K. Mitsuui, "Application of 100 MPa high strength, high fluidity concrete for prestressed concrete bridge with span-depth ratio

of 40," in *Proceedings of the PCI/FHWA International Syposium on High Performance Concrete*, vol. 10, pp. 669–680, New Orleans, La, USA, 1997.

[3] B. Persson, "Self-desiccation and its importance in concrete technology," *Materials and Structures*, vol. 30, no. 199, pp. 293–305, 1997.

[4] Q. Yang, "Inner relative humidity and degree of saturation in high-performance concrete stored in water or salt solution for 2 years," *Cement and Concrete Research*, vol. 29, no. 1, pp. 45–53, 1999.

[5] A. Loukili, A. Khelidj, and P. Richard, "Hydration kinetics, change of relative humidity, and autogenous shrinkage of ultra-high-strength concrete," *Cement and Concrete Research*, vol. 29, no. 4, pp. 577–584, 1999.

[6] O. M. Jensen, "Thermodynamic limitation of self-desiccation," *Cement and Concrete Research*, vol. 25, no. 1, pp. 157–164, 1995.

[7] A. Loukili, D. Chopin, A. Khelidj, and J.-Y. Le Touzo, "New approach to determine autogenous shrinkage of mortar at an early age considering temperature history," *Cement and Concrete Research*, vol. 30, no. 6, pp. 915–922, 2000.

[8] O. M. Jensen and P. F. Hansen, "Influence of temperature on autogenous deformation and relative humidity change in hardening cement paste," *Cement and Concrete Research*, vol. 29, no. 4, pp. 567–575, 1999.

[9] M. Lopez, L. F. Kahn, and K. E. Kurtis, "Effect of internally stored water on creep of high-performance concrete," *ACI Materials Journal*, vol. 105, no. 3, pp. 265–273, 2008.

[10] O. M. Jensen and P. Lura, "Techniques and materials for internal water curing of concrete," *Materials and Structures*, vol. 39, no. 293, pp. 817–825, 2006.

[11] L. F. Pang, S. Y. Ruan, and Y. T. Cai, "Effects of internal curing by super absorbent polymer on shrinkage of concrete," *Key Engineering Materials*, vol. 477, pp. 200–204, 2011.

[12] G. Barluenga, "Fiber-matrix interaction at early ages of concrete with short fibers," *Cement and Concrete Research*, vol. 40, no. 5, pp. 802–809, 2010.

[13] R. D. Toledo Filho, K. Ghavami, M. A. Sanjuán, and G. L. England, "Free, restrained and drying shrinkage of cement mortar composites reinforced with vegetable fibres," *Cement and Concrete Composites*, vol. 27, no. 5, pp. 537–546, 2005.

[14] Y. Chen, J. Wan, X. Zhang, Y. Ma, and Y. Wang, "Effect of beating on recycled properties of unbleached eucalyptus cellulose fiber," *Carbohydrate Polymers*, vol. 87, no. 1, pp. 730–736, 2012.

[15] S. Kawashima and S. P. Shah, "Early-age autogenous and drying shrinkage behavior of cellulose fiber-reinforced cementitious materials," *Cement and Concrete Composites*, vol. 33, no. 2, pp. 201–208, 2011.

[16] G. H. D. Tonoli, M. N. Belgacem, G. Siqueira, J. Bras, H. Savastano Jr., and F. A. Rocco Lahr, "Processing and dimensional changes of cement based composites reinforced with surface-treated cellulose fibres," *Cement and Concrete Composites*, vol. 37, no. 1, pp. 68–75, 2013.

[17] G. Xiuyan, J. Zhengwu, and M. Guojin, "Property evaluation of various lignocellulosic fibers from waste paper," *Journal of Harbin Engineering University*, vol. 36, no. 2, pp. 1–5, 2015.

[18] M. A. Nassar, N. A. Abdelwahab, and N. R. Elhalawany, "Contributions of polystyrene to the mechanical properties of blended mixture of old newspaper and wood pulp," *Carbohydrate Polymers*, vol. 76, no. 3, pp. 417–421, 2009.

[19] R. S. P. Coutts, "Wastepaper fibres in cement products," *International Journal of Cement Composites and Lightweight Concrete*, vol. 11, no. 3, pp. 143–147, 1989.

[20] J. Pe'rea, J. Ambroise, J. Biermann, and N. Voogt, "Use of thermally converted paper residue as a building material," in *Proceedings of the 3rd CANMET/ACI International Symposium on Sustainable Development of Cement and Concrete*, San Francisco, Calif, USA, September 2001.

[21] B. J. Mohr, H. Nanko, and K. E. Kurtis, "Durability of kraft pulp fiber-cement composites to wet/dry cycling," *Cement and Concrete Composites*, vol. 27, no. 4, pp. 435–448, 2005.

[22] X. Guo, Z. Jiang, H. Li, and W. Li, "Production of recycled cellulose fibers from waste paper via ultrasonic wave processing," *Journal of Applied Polymer Science*, vol. 132, no. 19, pp. 6211–6218, 2015.

[23] Chinese National Standard, *GB/T 17671: Method of Testing Cements-Determination of Strength*, Chinese National Standard, Beijing, China, 1999.

[24] Chinese National Standard, *JGJ/T 70: Standard for Test Method of Basic Properties of Construction Mortar*, Chinese National Standard, Beijing, China, 2009.

[25] P. Wang, Y. Peng, and X. Liu, "Comparison of methods for determination of hydration degree of polymer modified cement paste," *Journal of the Chinese Ceramic Society*, vol. 41, no. 8, pp. 1116–1123, 2013.

[26] M. Sarigaphuti, S. P. Shah, and K. D. Vinson, "Shrinkage cracking and durability characteristics of cellulose fiber reinforced concrete," *ACI Materials Journal*, vol. 90, no. 4, pp. 309–318, 1993.

[27] P. Soroushian and S. Ravanbakhsh, "Control of plastic shrinkage cracking with specialty cellulose fibers," *ACI Materials Journal*, vol. 95, no. 4, pp. 429–435, 1998.

[28] J. R. Rapoport and S. P. Shah, "Cast-in-place cellulose fiber-reinforced cement paste, mortar, and concrete," *ACI Materials Journal*, vol. 102, no. 5, pp. 299–306, 2005.

[29] J. Bijen, "Benefits of slag and fly ash," *Construction and Building Materials*, vol. 10, no. 5, pp. 309–314, 1996.

[30] S. Ahmad, "Reinforcement corrosion in concrete structures, its monitoring and service life prediction—a review," *Cement and Concrete Composites*, vol. 25, no. 4-5, pp. 459–471, 2003.

[31] C. Wang, C. Yang, J. Qian, M. Zhong, and S. Zhao, "Behavior and mechanism of pozzolanic reaction heat of fly ash and ground granulated blastfurnace slag at early age," *Journal of the Chinese Ceramic Society*, vol. 40, no. 7, pp. 1050–1058, 2012.

[32] S. Wei and J. A. Mandel, "Effects of fiber spacing on interfacial layers," *Journal of the Chinese Ceramic Society*, vol. 17, no. 3, pp. 266–271, 1989.

[33] O. M. Jensen and P. F. Hansen, "Water-entrained cement-based materials—I. Principles and theoretical background," *Cement and Concrete Research*, vol. 31, no. 4, pp. 647–654, 2001.

[34] O. M. Jensen and P. F. Hansen, "Water-entrained cement-based materials: II. Experimental observations," *Cement and Concrete Research*, vol. 32, no. 6, pp. 973–978, 2002.

[35] A. Ming-zhe, Z. Jin-quan, and Q. Wei-zu, "Autogenous shrinkage of high performance concrete," *Journal of Building Materials*, vol. 4, no. 2, pp. 159–166, 2001.

[36] D. P. Bentz, M. R. Geiker, and K. K. Hansen, "Shrinkage-reducing admixtures and early-age desiccation in cement pastes and mortars," *Cement and Concrete Research*, vol. 31, no. 7, pp. 1075–1085, 2001.

[37] X. Kong and Q. Li, "Influence of super absorbent polymer on dimension shrinkage and mechanical properties of cement mortar," *Journal of the Chinese Ceramic Society*, vol. 37, no. 5, pp. 855–861, 2009.

[38] H. Shu-Guang, Z. Yu-Fei, and W. Fa-Zhou, "Temperature controlling and monitoring for mass concrete construction of Huangpu bridge," *Journal of Huazhong University of Science and Technology*, vol. 25, no. 1, pp. 1–4, 2008 (Chinese).